MIXED CONDUCTOR-CONTAINING ANODES OF SOLID OXIDE FUEL CELLS

E.V. Tsipis, V.V. Kharton and J.R. Frade*

Department of Ceramics and Glass Engineering, CICECO, University of Aveiro, 3810-193 Aveiro, Portugal

* Corresponding author. Fax: +351-234-425300; Tel: +351-234-370254; E-mail: jfrade@cv.ua.pt

ABSTRACT

Developments of intermediate-temperature solid oxide fuel cells (IT SOFCs) require novel anode materials with high electrochemical activity at 800-1070 K. In order to assess the role of oxide components of Ni- and Cu-containing cermets, a series of electrodes containing 8% yttria-stabilized zirconia (Y8SZ), $Ce_{0.8}Gd_{0.2}O_{2-\delta}$ (CGO) and $TbZrO_{4-\delta}$ with fluorite-related structure, zircon-type $Ce_{0.8}Ca_{0.2}VO_{4+\delta}$, pyrochlore $Gd_{1.86}Ca_{0.14}Ti_2O_{7-\delta}$ (GCTO), and $La_{0.9}Sr_{0.1}Al_{0.65}Mg_{0.15}Fe_{0.20}O_{3-\delta}$ perovskite, were studied in contact with $(La_{0.9}Sr_{0.1})_{0.98}Ga_{0.8}Mg_{0.2}O_{3-\delta}$ (LSGM) electrolyte. The best performance was found for anodes comprising a stable ion-conducting component, such as Y8SZ or GCTO, and one Ce-containing phase, such as CGO or cerium vanadate. Anode performance is less dependent on the ionic conductivity of oxide components than on redox stability or interaction between different cell materials. Surface modification with ceria substantially reduces overpotentials of all cermet anodes. For Ni-CGO and Cu-CGO, such activation of yields about 100-115 mV at 1073 K and 200 mA/cm^2 in 10%H_2-90%N_2, for both anodes.

(Comment: it might be important to use the word "overpotential", as "polarization" is usually a qualitative term)

Keywords: B. composites, C. Electrical properties, C. ionic conductivity, E. Fuel cells, Cermet anode

INTRODUCTION

Developments of intermediate-temperature solid oxide fuel cells (IT SOFCs) require optimization of anode compositions and microstructure to achieve sufficiently low overpotentials at 773 - 1073 K.[1,2] Incorporation of catalytically-active pure or doped ceria was proved to enhance the performance of conventional anode cermets, consisting of metallic Ni and 8mol%-yttria-stabilized zirconia (Y8SZ).[1-5] Though Y8SZ plays a stabilizing role with respect to redox cycling and Ni sintering under the anode operation conditions,[4] improved electrode kinetics could be expected by partial or complete substitution by other oxide materials having higher electrocatalytic activity and/or mixed conductivity. Attention has also been given to Cu-based anodes, due to its lower catalytic activity for C-C bond formation[5,6], thus suppressing the deposition of carbon on cermet anodes of hydrocarbon-fueled SOFCs.

The present study is centered on the effects of mixed-conducting oxide components on the performance of Ni- and Cu-containing anodes in contact with $(La_{0.9}Sr_{0.1})_{0.98}Ga_{0.8}Mg_{0.2}O_{3-\delta}$ (LSGM) solid electrolyte.

EXPERIMENTAL

Ni-containing cermets was prepared, namely Ni - Y8SZ – $Ce_{0.8}Gd_{0.2}O_{2-\delta}$ (CGO), Ni - $Gd_{1.86}Ca_{0.14}Ti_2O_{7-\delta}$ - CGO, Ni -Y8SZ -$Ce_{0.8}Ca_{0.2}VO_{4+\delta}$, Ni -$Tb_{0.5}Zr_{0.5}O_{2-\delta}$ -CGO and Ni - $La_{0.90}Sr_{0.10}Al_{0.65}Fe_{0.20}Mg_{0.15}O_{3-\delta}$ - CGO, with phase weight ratios 50:30:20%. The Ni-phase was first added as NiO, by thermal decomposition of $Ni(NO_3)_2{\cdot}6H_2O$, and later reduced to Ni. Submicron powders of CGO, $Tb_{0.5}Zr_{0.5}O_{2-\delta}$ and $La_{0.90}Sr_{0.10}Al_{0.65}Fe_{0.20}Mg_{0.15}O_{3-\delta}$ were synthesized via the cellulose-precursor technique,[3] mechanically-activated synthesis[7] and glycine-nitrate process[8], respectively. $Gd_{1.86}Ca_{0.14}Ti_2O_{7-\delta}$ (GCTO) and $Ce_{0.8}Ca_{0.2}VO_{4+\delta}$ were synthesized by powder reactions[9,10] with subsequent ball-milling. Commercial Y8SZ powder (Tosoh) was used for preparation of theese cermets. In addition, Ni - CGO (25 – 75 wt% or 50 – 50 mol%) and Cu - CGO (27 – 73 wt% or 50 – 50 mol%) cermets were prepared via the cellulose-precursor method. In this case, oxide fibers retain a texture of initial cellulose precursor (Fig.1A) and easily transform to homogeneous nanocrystalline powders (Fig.1B). Phase composition was verified by X-ray diffraction (XRD) and transmission electron microscopy (TEM). Transport properties of the mixed-conducting ceramic materials were studied by measurements of faradaic efficiency, e.m.f. of oxygen concentration cells, and total conductivity and Seebeck coefficient vs. oxygen partial pressure, as described earlier. [7,9,10] Electrode layers with 15-25 mg/cm^2 were screen-printed onto the surface of dense LSGM ceramics and annealed in air for 2 h; the sintering temperature was 1523 K for Ni - Y8SZ - CGO, 1273 K for Cu-containing cermet and 1573 K in all other

cases. The anodic overpotential (η) as function of current density (i) was studied by the 3-electrode technique, with Pt counter and reference electrodes; according to the cell geometry reported in Ref.11. The polarization measurements were performed using an AUTOLAB PGSTAT20 at 873-1073 K in flowing wet 10%H_2-90%N_2 gas mixture, $p(O_2)$ being controlled by an oxygen sensor. After the electrochemical tests, selected anodes were surface-modified by impregnation with saturated $Ce(NO_3)_3 \cdot 6H_2O$ solution in ethanol, followed by annealing at 1073-1273 K; then the overpotential-current dependencies were re-measured. Details of experimental procedures and equipment were published elsewhere.[3,7,9,10]

Results and Discussion

Fig.2 presents selected overpotential-current dependencies of the mixed conductor-containing anodes. Compared to other layers without surface modification, the best performance was found for Ni - Y8SZ - CGO, Ni - Y8SZ - $Ce_{0.8}Ca_{0.2}VO_{4+\delta}$ and Ni - GCTO - CGO compositions. The electrochemical activity of Ni - $Tb_{0.5}Zr_{0.5}O_{2-\delta}$ - CGO and Ni - $La_{0.90}Sr_{0.10}Al_{0.65}Fe_{0.20}Mg_{0.15}O_{3-\delta}$ - CGO layers is rather poor. The Ni-CGO anode exhibits lower overpotentials with respect to the Cu-containing analogue; this behavior is generally associated with low catalytic activity and high sinterability of copper.[5,6] Surface modification considerably increases the performance, yielding similar results for both anodes. For example, the overpotentials are about 80 mV at 1073 K and 150 mA/cm^2 for both Ni-CGO and Co-CGO anodes activated with ceria.

Fig.3 summarizes the data on transport properties of the ion-conducting oxide components. The values of total conductivity (σ) correspond to $p(O_2) = 10^{-20}$ atm, which is close to SOFC anode operation conditions. Transport number measurements are often performed only for oxidizing conditions, due to experimental limitations, and the ionic conductivity (σ_o) data shown in Fig.3 thus refers to $p(O_2)$=0.21 atm. Although σ_o is often $p(O_2)$-dependent and the actual values should not be used for quantitative analysis under different conditions, their comparison may still be useful to identify basic trends. In particular, despite the highest ionic conductivity of CGO, the electrodes Ni - Y8SZ - CGO, Ni - Y8SZ - $Ce_{0.8}Ca_{0.2}VO_{4+\delta}$ and Ni - GCTO - CGO show similar performance (Fig.2). The electronic conductivity of oxide components of Ni- or Cu-based cermets has no essential effect on the overall performance, with current collection being ensured by the metal. (Comment: if electrocatalytic activity would be significantly dependent on electronic transport, we would have maximum performance for CeVO4). On the contrary, alternative ceramic anodes should include a component with high electronic conductivity.

The results thus suggest that, for cases when sufficient levels of ionic and electronic conduction are attained in cermet anodes, further increase in transport properties is less important than stability with respect to coarsening of metal particles, interactions between cell materials or volume changes under anode working conditions. Stability is expected for oxide phases with essentially $p(O_2)$-independent oxygen stoichiometry, including Y8SZ and GCTO. Surface activation of Ni - GCTO - CGO anodes thus lowers the overpotentials by 3-5 times at 1073 K, and is more effective for Ni-CGO anodes than for Ni-GCTO-CGO (Fig.2), possibly due to greater volume changes on varying redox conditions for the former composition. Volume changes are likely to affect the contacts at electrode/electrolyte interface or contacts between grains of different anode components.

Though the presence of Ce-containing phases with different composition and transport properties, (e.g. CGO and $Ce_{0.8}Ca_{0.2}VO_{4+\delta}$) may provide similar electrochemical activity, the electrode performance may be affected by reactive layers between $Ce_{0.8}Ca_{0.2}VO_{4+\delta}$ and LSGM (Fig.1D). Poorer performance was also obtained on adding $Tb_{0.5}Zr_{0.5}O_{2-\delta}$ (Fig.2B), possibly due to chemical interaction between $Tb_{0.5}Zr_{0.5}O_{2-\delta}$ and CGO, as revealed by XRD (Fig.4A). On the contrary, no reaction was detected between components of Ni - $La_{0.90}Sr_{0.10}Al_{0.65}Fe_{0.20}Mg_{0.15}O_{3-\delta}$-CGO anodes (Fig.4B). Thus, high overpotentials of these anodes on LSGM are probably related to large changes in oxygen nonstoichiometry of the Fe-containing phase, or cation interdiffusion between $La_{0.90}Sr_{0.10}Al_{0.65}Fe_{0.20}Mg_{0.15}O_{3-\delta}$ and LSGM. For example, incorporation of Al^{3+} cations into the LSGM surface may lower its ionic conduction, and Fe diffusion may cause microcracks on varying the local conditions of oxygen chemical potential and/or overpotential/current changes.

In summary, the results of this work show that redox stability is required to retain the positive role of mixed conducting components of cermet anodes for IT SOFCs. Ce-containing anode components are often effective, but further activation can be attained by impregnating with a ceria-based solution, yielding increased catalytic activity, improved intergranular contacts and, possibly also enhanced electronic conduction at the electrolyte surface.

Acknowledgements

This work was supported by the FCT, Portugal (projects POCTI/CTM/3938/2001 and BD/6827/2001), by the NATO Science for Peace program (project 978002). Helpful discussions and experimental contributions by I.A. Bashmakov, A.A. Yaremchenko and A.V. Shlyakhtina, are acknowledged.

References

1. Ishihara, T., Shibayama, T., Nishiguchi, H. and Takita, Y., Nickel–Gd-doped CeO_2 cermet anode for intermediate temperature operating solid oxide fuel cells using $LaGaO_3$-based perovskite electrolyte. *Solid State Ionics*, 2000, **132**, 209-216.
2. Watanabe, M., Uchida, H. and Yoshida, M., Effect of Ionic Conductivity of Zirconia Electrolytes on the Polarization Behavior of Ceria-Based Anodes in Solid Oxide Fuel Cells. *J. Electrochem. Soc.*, 1997, **144**, 1739-1743.
3. Kharton, V.V., Naumovich, E.N., Tikhonovich, V.N., Bashmakov, I.A., Boginsky, L.S. and Kovalevsky, A.V., Testing tubular solid oxide fuel cells in nonsteady-state conditions. *J. Power Sources*, 1999, **79**, 242-249.
4. Marina, O.A., Bagger, C., Primdahl, S. and Mogensen, M., A solid oxide fuel cell with a gadolinia-doped ceria anode: preparation and performance. *Solid State Ionics*, 1999, **123**, 199-208.
5. Gorte, R.J., Park, S., Vohs, J.M. and Wang, C., Anodes for direct oxidation of dry hydrocarbons in a solid-oxide fuel cell. Adv. Mater., 2000, **12**, 1465-1469.
6. Kim, H., Lu, C., Worrell, W.L., Vohs, J.M. and Gorte, J.R., Cu-Ni cermet anodes for direct oxidation of methane in solid-oxide fuel cells. *J. Electrochem. Soc.*, 2002, **149**, A247-A250.
7. Tsipis, E.V., Shlyakhtina, A.V., Shcherbakova, L.G., Kolbanev, I.V., Kharton, V.V., Vyshatko, N.P. and Frade, J.R., Mechanically-activated synthesis and mixed conductivity of $TbMO_{4-\delta}$ (M = Zr, Hf) ceramics. *J. Electroceram.*, 2003, **10**, 153-164.
8. Chick, L.A., Pederson, L.R., Maupin, G.D., Bates, J.L., Thomas, L.E. and Exarhos, G.L., Glycine-nitrate combustion synthesis of oxide ceramic powders. *Mater. Lett.*, 1990, **10**, 6-12.
9. Kharton, V.V., Tsipis, E.V., Yaremchenko, A.A., Vyshatko, N.P., Shaula, A.L., Naumovich, E.N. and Frade, J.R., Oxygen ionic and electronic transport in $Gd_{2-x}Ca_xTi_2O_{7-\delta}$ pyrochlores. *J. Solid State Electrochem.*, 2003, **7**, 468-476.
10. Tsipis, E.V., Kharton, V.V., Vyshatko, N.P., Shaula, A.L., and Frade, J.R., Stability and oxygen ionic conductivity of zircon-type $Ce_{1-x}A_xVO_{4+\delta}$ (A = Ca, Sr). *J. Solid State Chem.*, 2003, **176**, 47-56.
11. Mizusaki, J., Tagawa, H., Isobe, K., Tajika, M., Koshiro, I., Maruyama, H., and Hirano, K., Kinetics of the Electrode Reaction at the H_2-H_2O Porous Pt/ Stabilized Zirconia Interface. *J. Electrochem. Soc.*, 1994, **141**, 1674-1683.

FIGURE CAPTIONS

Fig.1. SEM micrograph (A) and bright-field TEM image and electron diffraction pattern (B) of Cu - CGO cermet prepared by cellulose-precursor technique and annealed in air at 1173 K; as-prepared and surface-modified Ni -GCTO - CGO anodes (C, right and left); as-prepared Ni - Y8SZ - $Ce_{0.8}Ca_{0.2}VO_{4+\delta}$ CGO layer in contact with LSGM (D).

Fig.2. Overpotential versus current density for various cermet anodes.

Fig.3. Ionic conductivity in air (A) and total conductivity at $p(O_2)=10^{-20}$ atm (B) for Y8SZ, $Ce_{0.8}Gd_{0.2}O_{2-\delta}$, $TbZrO_{4-\delta}$, $Ce_{0.8}Ca_{0.2}VO_{4+\delta}$, $Gd_{1.86}Ca_{0.14}Ti_2O_{7-\delta}$ and $La_{0.90}Sr_{0.10}Al_{0.65}Fe_{0.20}Mg_{0.15}O_{3-\delta}$.

Fig.4. XRD patterns of $Ce_{0.8}Gd_{0.2}O_{2-\delta}$, $TbZrO_{4-\delta}$ and oxidized Ni - $Tb_{0.5}Z_{0.5}rO_{2-\delta}$ - CGO layer (A), and the oxidized and reduced layers containing $La_{0.90}Sr_{0.10}Al_{0.65}Fe_{0.20}Mg_{0.15}O_{3-\delta}$ perovskite (B).

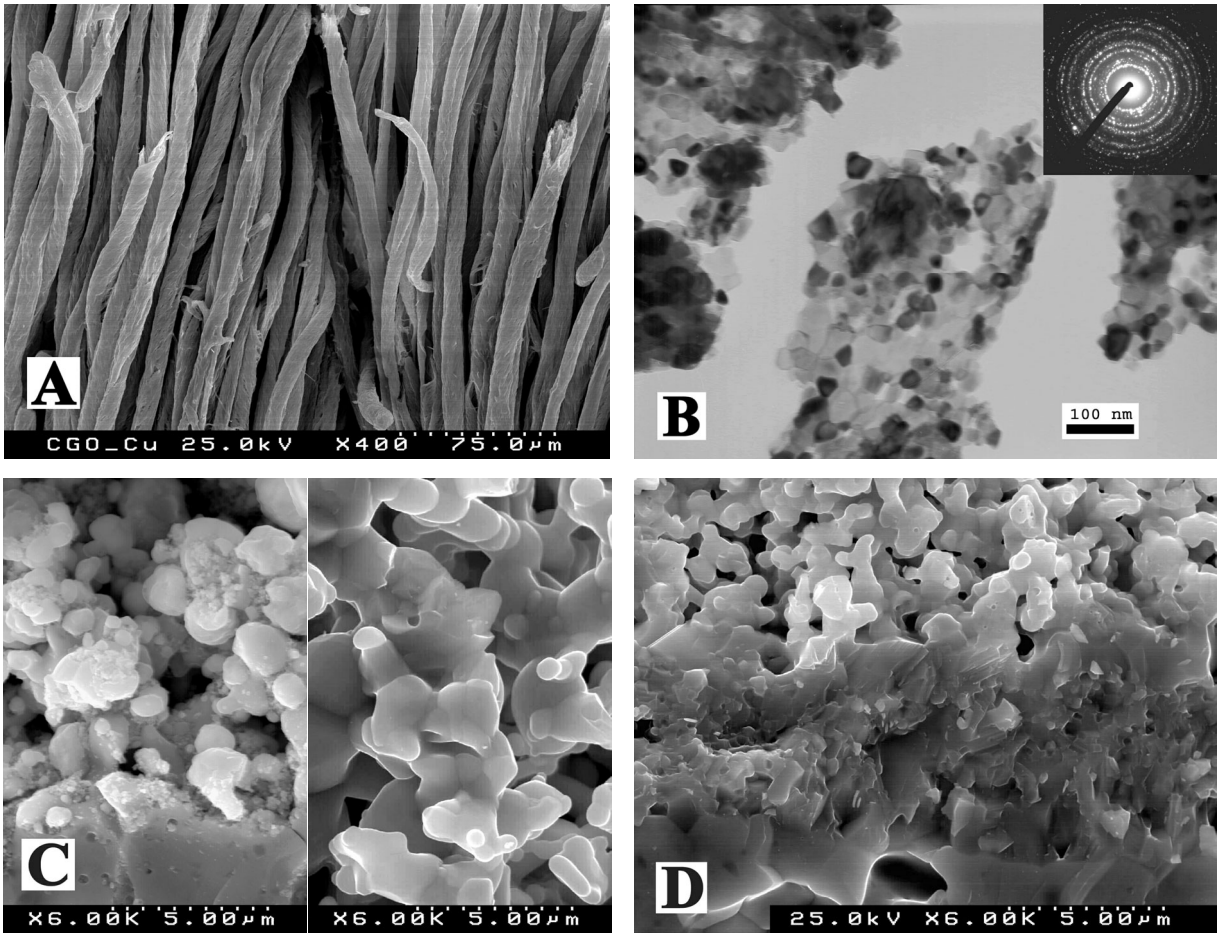
A
CGO_Cu 25.0kV X400 75.0µm
B
100 nm
C
X6.00K 5.00µm
X6.00K 5.00µm
D
25.0kV X6.00K 5.00µm

Fig.1

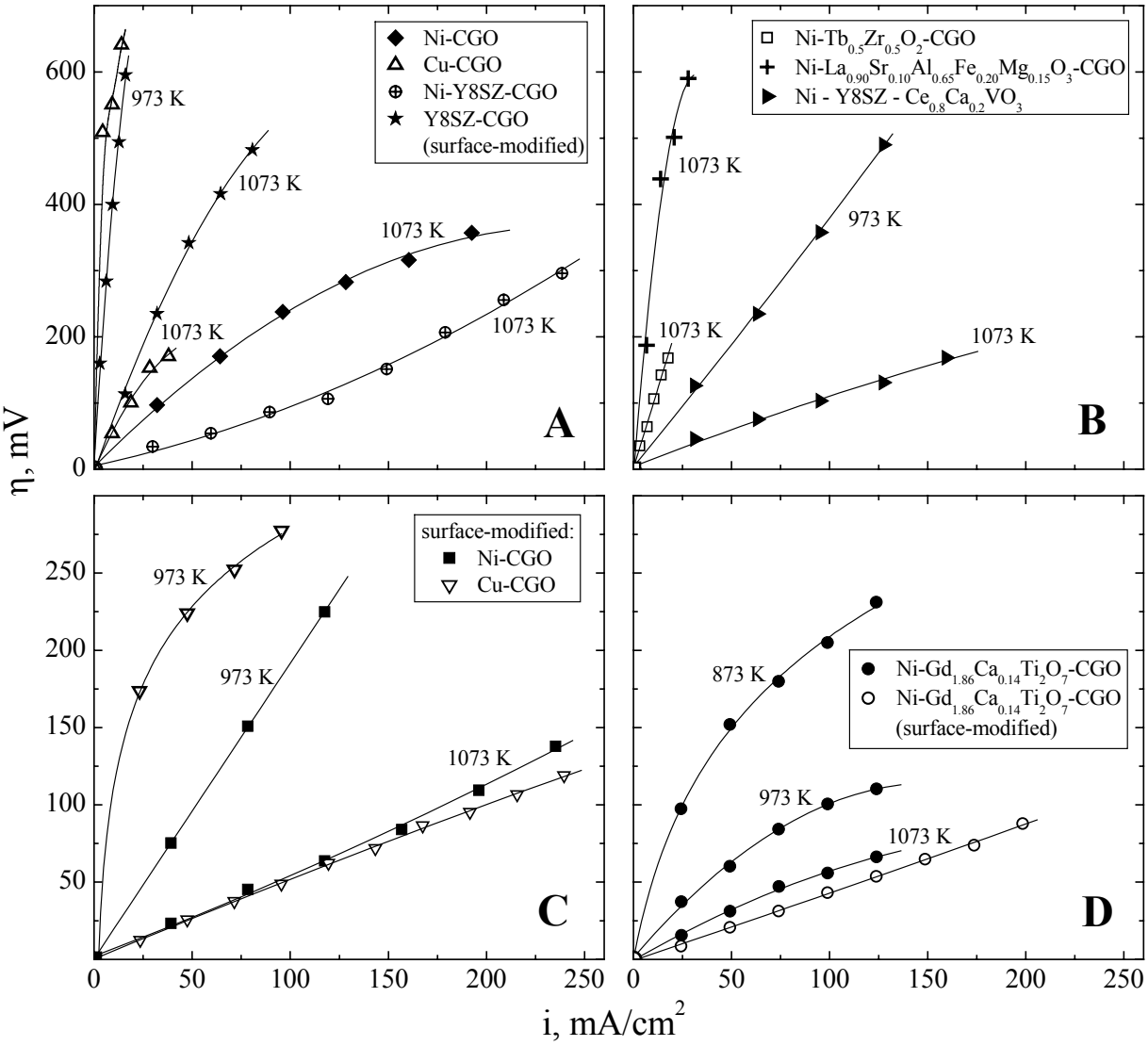
Ni-CGO
Cu-CGO
Ni-Y8SZ-CGO
Y8SZ-CGO
(surface-modified)
973 K
1073 K
1073 K
1073 K
1073 K
A
Ni-Tb0.5Zr0.5O2-CGO
Ni-La0.90Sr0.10Al0.65Fe0.20Mg0.15O3-CGO
Ni - Y8SZ - Ce0.8Ca0.2VO3
1073 K
973 K
1073 K
1073 K
B
surface-modified:
Ni-CGO
Cu-CGO
973 K
973 K
1073 K
C
Ni-Gd1.86Ca0.14Ti2O7-CGO
Ni-Gd1.86Ca0.14Ti2O7-CGO
(surface-modified)
873 K
973 K
1073 K
D
η, mV
i, mA/cm2
0
50
100
150
200
250
400
600

Fig.2

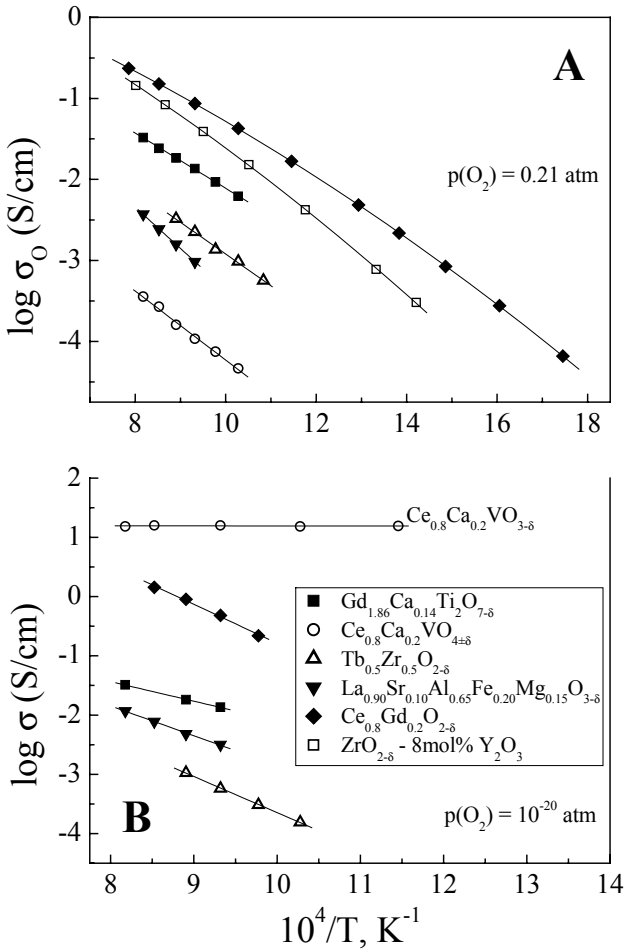
A
p(O2) = 0.21 atm
log σO (S/cm)
B
p(O2) = 10-20 atm
Ce0.8Ca0.2VO3-δ
Gd1.86Ca0.14Ti2O7-δ
Ce0.8Ca0.2VO4±δ
Tb0.5Zr0.5O2-δ
La0.90Sr0.10Al0.65Fe0.20Mg0.15O3-δ
Ce0.8Gd0.2O2-δ
ZrO2-δ - 8mol% Y2O3
log σ (S/cm)
10^4/T, K^-1

Fig.3

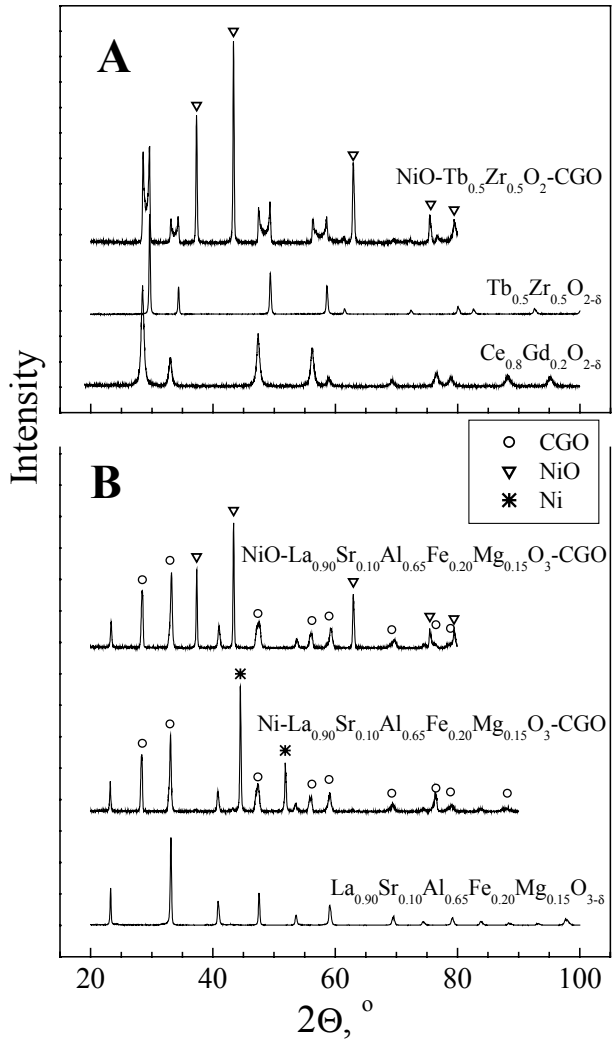
A
NiO-Tb0.5Zr0.5O2-CGO
Tb0.5Zr0.5O2-δ
Ce0.8Gd0.2O2-δ
B
CGO
NiO
Ni
NiO-La0.90Sr0.10Al0.65Fe0.20Mg0.15O3-CGO
Ni-La0.90Sr0.10Al0.65Fe0.20Mg0.15O3-CGO
La0.90Sr0.10Al0.65Fe0.20Mg0.15O3-δ
Intensity
20
40
60
80
100
2Θ, o

Fig.4